

## Wodginite and associated oxide minerals from the Peerless pegmatite, Pennington County, South Dakota

P. ČERNÝ

*Department of Earth Sciences, University of Manitoba  
Winnipeg, Manitoba, Canada R3T 2N2*

W. L. ROBERTS

*Department of Geology  
South Dakota School of Mines and Technology  
Rapid City, South Dakota 57701*

T. S. ERCIT AND R. CHAPMAN

*Department of Earth Sciences, University of Manitoba  
Winnipeg, Manitoba, Canada R3T 2N2*

### Abstract

Wodginite occurs in one of the intermediate albite-rich units of the Peerless pegmatite, near Keystone, Pennington County, South Dakota. It is associated with cassiterite containing exsolved tantalite and tapiolite, and with microlite. The chemical composition of wodginite varies from  $(\text{Mn}_{3.45}\text{Fe}_{0.40})(\text{Sn}_{3.16}\text{Ta}_{0.55}\text{Fe}_{0.23}^{3+}\text{Ti}_{0.06}) (\text{Ta}_{6.86}\text{Nb}_{1.14})\text{O}_{32}$  to  $\text{Mn}_{3.99}(\text{Sn}_{3.31}\text{Ta}_{0.45}\text{Fe}_{0.10}^{3+}\text{Ti}_{0.07}) (\text{Ta}_{7.18}\text{Nb}_{0.82})\text{O}_{32}$ . With decreasing total iron, the color of wodginite changes from black to pale cinnamon brown. The markedly monoclinic unit cell dimensions ( $a$  9.533–9.552,  $b$  11.471–11.476,  $c$  5.116–5.123 Å,  $\beta$  90.8–91.2°,  $V$  559.4–561.5 Å<sup>3</sup>) suggest a well-ordered structure. Wodginite and associated microlite seem to be the final precipitates in a sequence ferrocolumbite → manganocolumbite → manganotantalite → wodginite → microlite. Fractionation progresses in this sequence from 0.07 to  $\geq 0.93$  in  $\text{Ta}/(\text{Ta} + \text{Nb})$  and from 0.39 to  $\geq 0.99$  in  $\text{Mn}/(\text{Mn} + \text{Fe})$ .

### Introduction

To date, wodginite has been reported from at least 30 worldwide localities, but until recently this mineral has not been recorded in the United States. The first U.S. occurrences were discovered in the Black Hills of South Dakota in 1979, as described in the present paper, and in the Herbb no. 2 pegmatite, Virginia in 1981 (Wise and Černý, 1984).

### The parent pegmatite

The Peerless pegmatite near Keystone, Pennington County, South Dakota is one of the more fractionated and internally complex pegmatites of the northern margin of the pegmatite field of the southern Black Hills. According to Sheridan et al. (1957), the pegmatite has an anticlinal shape, with a subhorizontal NW-trending crest flanked by SW- and NE-dipping limbs. The outcrop is about 185 × 110 m in size. Three major keels and several minor rolls complicate the apparently fracture-controlled underside of the pegmatite, whereas the crest is relatively simple, consisting essentially of two subparallel bulges. Internally, the pegmatite consists of 7 zones, 2 replacement units and 2 types of fracture-filling units. A detailed description of the

morphology and internal structure is provided by Sheridan et al. (1957).

The Peerless pegmatite was a major source of feldspars, scrap mica, beryl and amblygonite-montebbrasite during the first half of the 20th century. Punch and sheet mica, columbite-tantalite and cassiterite were minor byproducts.

Petrologically, the Peerless represents a rare example of a phosphorus-rich lithium pegmatite which contains all Li bound in primary phosphates (particularly as huge quantities of amblygonite-montebbrasite) to the virtual exclusion of anhydrous Li-aluminosilicates (cf. Burt and London, 1982 for the phase relationships).

A number of different minerals has been reported from this pegmatite: plagioclase, quartz, muscovite varieties, microcline-perthite and microcline are the most abundant rock-forming minerals; beryl, tourmaline, triphylite, amblygonite-montebbrasite, apatite, columbite-tantalite and cassiterite are subordinate to accessory phases; minor to rare mineral species include garnet, biotite, zircon, spodumene, uraninite, chrysoberyl, tantalum rutile, opal, pyrolusite, goethite, triplodite(?), carbonate-apatite, vivianite, ferri-sicklerite, heterosite, libethenite, pseudomalachite, goyazite, autunite, torbernite, siderite, malachite, azurite, loell-

ingite(?), pyrite, marcasite, stannite and kesterite. During the present study, wodginite, microlite and tapiolite have been added to this list.

The Peerless pegmatite is a Na, P, F-enriched rare-element pegmatite, with Li, Be and subordinate Nb, Ta, Sn mineralization, and modest enrichment in Rb and Cs. The K/Rb and K/Cs ratios reach 25.5 and 740 respectively in the K-feldspars of intermediate zones, 18 and 420 in muscovite of intermediate zones, and 13.2 and 385 in late, slightly Li-enriched muscovite of the central parts of the pegmatite (0.35 wt.% Li<sub>2</sub>O). Beryl also shows increased contents of Li<sub>2</sub>O (≤ 1.10 wt.%) and Cs<sub>2</sub>O (≤ 1.05 wt.%).

**Paragenetic relationships of wodginite**

Wodginite was found in the cleavelandite fringe of an albitic unit exposed in the northeastern, partly overhanging wall of the main pegmatite quarry, very close to the E-E' section line of Sheridan et al. (1957, Plate 4). The cleavelandite fringe which contains intergrown muscovite is located along the contact of the albitic unit with an underlying mass of quartz. Section E-E' in Sheridan et al. (1957, Plate 6) indicates that the present exposure corresponds to a segment of quartz zone 6b overlain by the 3rd intermediate cleavelandite + quartz zone 5, as designated by these authors.

Because of the relative abundance of columbite-tantalite and cassiterite in the wodginite-bearing albitic unit, representative specimens of these minerals were collected over the accessible width of this unit, and examined in order to establish the general paragenetic and geochemical environment in which the wodginite occurs. The different mineral associations are listed in Table 1, letter-coded in the sequence of their occurrence from inside the albitic unit toward the massive quartz zone.

**Experimental methods**

All chemical analyses were done with an MAC 5 electron microprobe operating in both wavelength-dispersive (WD) and energy-dispersive (ED) modes. Standards used were cassiterite (SnLα), chromite (FeKα), sphene (TiKα), manganotantalite (MnKα, TaLα, Mα), Ba<sub>2</sub>NaNb<sub>5</sub>O<sub>15</sub> and CaNb<sub>2</sub>O<sub>6</sub> (NbLα). Conditions of analysis were: accelerating potentials of 20, 15 kV, sample currents of 40 nA (WD) and 5 nA (ED) measured on brass (WD) and ZnS (ED), count times of 10 s (WD) and 200 live seconds (ED). Wavelength-dispersive spectral data were reduced with the program EMPADR VII (Rucklidge Gasparrini, 1969). Energy-dispersive spectra were collected with a KEVEX Model 7000 ED spectrometer and were reduced with KEVEX software utilizing the program MAGIC V (Colby, 1980). Peak overlap problems encountered during analysis of ED spectra were resolved by stripping techniques involving library spectra.

Most unit cell dimensions were calculated from X-ray powder diffraction data obtained with Philips X-ray diffractometers using Ni-filtered or graphite-monochromated CuKα radiation (λ = 1.5418Å) and scanning speeds of 1/4 to 1/2° 2θ/min. A minimum of 10 and a maximum of 33 reflections measured between 10° and 70° 2θ were used in least-squares refinement of the data. Annealed CaF<sub>2</sub> (a = 5.4620Å) was used as an internal calibration standard. Wodginite sample D1(w) (Table 1) was the only exception to this

Table 1. The examined associations of Nb, Ta, Sn-bearing minerals from the Peerless Pegmatite

Association A: platy columbite (1-6 mm thick, 3-80 cm across) studded with zircon, in cleavelandite; samples A1(ct) to A5(ct).
Association B: thick tabular columbite-tantalite (5 to 60 mm in maximum dimension) in coarse-grained albite and cleavelandite, with subordinate muscovite; samples B1(ct) to B4(ct).
Association C: coarse-grained anhedral cassiterite (5 to 120 mm) with exsolved columbite-tantalite and tapiolite, in cleavelandite + muscovite adjacent to massive quartz; samples
C1(c) with exsolved C1(ct)
C2(c) with exsolved C2(ct)
C3(c) with exsolved C3(t)
C4(c) with exsolved C4(t)
Association D: wodginite (divergent columnar aggregate 50 mm long) with inclusions and/or exsolutions of cassiterite, microlite and tapiolite, in cleavelandite + muscovite adjacent to massive quartz; samples
D1(w) black-brown with overgrowth of D1(t), and D1(c) with exsolved D1(ct)
D2(w) brown
D3(w) pale brown with D3(c) and D3(m)
A, B, C, D - mineral associations; 1, 2, 3, ... - samples within each mineral association; ct - columbite-tantalite, c - cassiterite, w - wodginite, t - tapiolite, m - microlite.

procedure; because of the lack of material, it was X-rayed in a Gandolfi camera and the film data were corrected for shrinkage. In all cases, the program CELREF (Appleman and Evans, 1973) was used for unit cell refinement.

In the heating experiments, separate fragments 0.5 to 2 mm in size were extracted from the samples and were heated in air at 1000°C for 16 hours. Heating relatively coarse-grained material minimizes oxidation of Fe<sup>2+</sup> to such a degree that unit cell dimensions of columbites-tantalites heated in air and in controlled atmosphere (CO/CO<sub>2</sub> = 2.5/1) are statistically identical (unpubl. data of Černý and Turnock).

**Mineralogy**

*Wodginite*

The divergent cluster of subhedral and somewhat skeletal wodginite crystals is black at the point of spreading, grading into medium-brown and turning pale cinnamon-brown at the diverging crystal terminations. The black point of the cluster contains cassiterite grains with microscopic tantalite inclusions, and microgranular tapiolite along contacts of cassiterite with wodginite. Intermediate parts of the wodginite cluster are not associated with other phases; however, the diverging wodginite terminations contain exsolved cassiterite, and euhedral crystals of pale gray microlite along wodginite contacts with albite.

In general, the wodginite composition is close to the ideal formula MnSnTa<sub>2</sub>O<sub>8</sub>, particularly in the diverging pale-brown terminations (association D, Table 1, Fig. 1). Analyses D1w and D3w are among the most Sn-rich compositions found in wodginites (unpubl. data of T.S.E. and P.Č.). In the (Nb, Ta)O<sub>2.5</sub>-(Fe, Mn)O-(Sn, Ti)O<sub>2</sub> diagram,

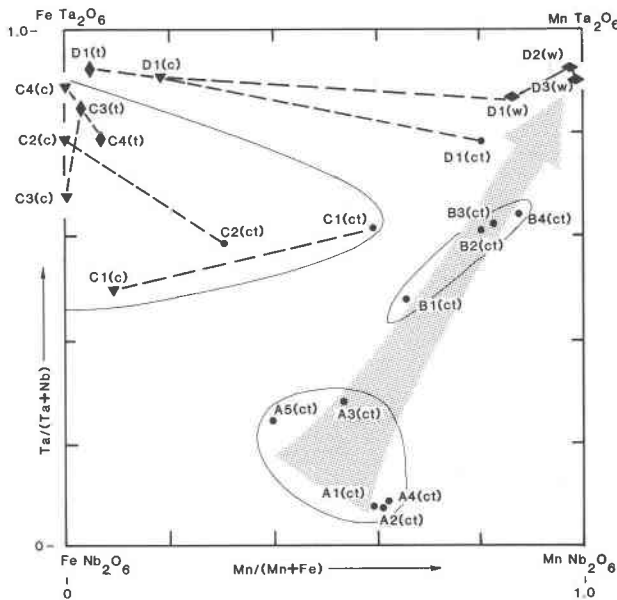


Fig. 1. Compositions of the examined minerals in the columbite-tantalite (-tapiolite) quadrilateral. Dots—columbite-tantalite; horizontal diamonds—wodginite; upright diamonds—tapiolite; triangles—cassiterite. Dashed lines connect coexisting minerals; thin lines encircle individual mineral associations characterized in Table 1; the arrow shows the general fractionation trend as described in the text.

wodginite compositions plot very close to the ideal substitution trend  $(\text{Fe, Mn})^{2+} + 2(\text{Nb, Ta})^{5+} \rightleftharpoons 3(\text{Sn, Ti})^{4+}$  (Fig. 2), which joins ideal columbite-tantalite with the (Sn, Ti) corner. However, this plot is somewhat unrealistic for wodginite because wodginite includes minor  $\text{Fe}^{3+}$  with  $\text{Fe}^{2+}$ .

Site assignments were made according to the present understanding of the crystal chemistry of wodginite (Ferguson et al. 1976; Ercit, Černý and Hawthorne, in prep.) and its recently expanded compositional variability (Černý and Ercit, 1985).  $\text{Mn}^{2+}$  was assigned to the A-site, all Nb and Ta = (8-Nb) were assigned to the B-site and Ti, Sn and excess Ta from the B-site calculations were assigned to the C-site.  $\text{Fe}^{2+} : \text{Fe}^{3+}$  was calculated from the total iron of analysis by assuming all iron in the A-site to be ferrous and all iron in the C-site to be ferric, in analogy to the results of wet chemical analyses of other samples (von Knorring et al. 1969) and on site charge and size considerations (Ferguson et al. 1976). In such calculations it is important to consider the distribution of cation site vacancies (Graham and Thorner, 1974). Vacancies are incorporated as part of an attempt to achieve charge balance, necessitated by excess positive charge introduced by  $\text{Sn}^{4+} \rightarrow \text{Ta}^{5+}$  substitution at the C-site. As such, vacancies should be preferentially, although not necessarily exclusively, incorporated into the adjacent A-site, to satiate local bond valence requirements (Ercit, Černý and Hawthorne, in prep.). In calculations where the A-site could not accommodate all vacancies, the

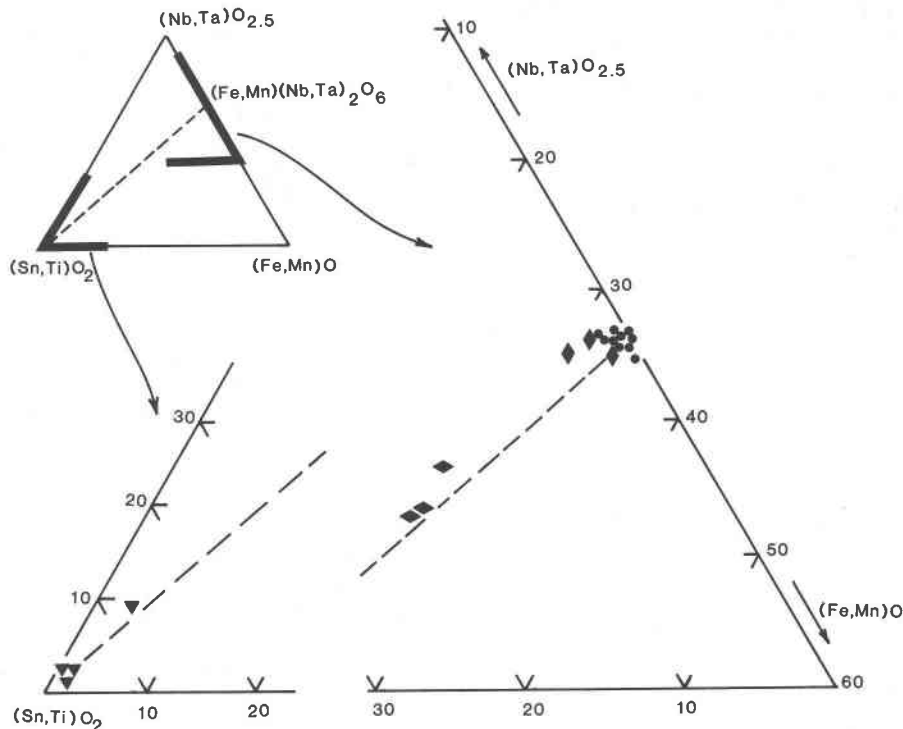
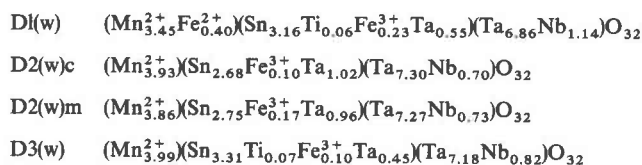


Fig. 2. Compositions of the examined minerals in the  $(\text{Sn, Ti})\text{O}_2$ — $(\text{Nb, Ta})\text{O}_{2.5}$ — $(\text{Fe, Mn})\text{O}$  triangle. Symbols as in Fig. 1. Dashed lines mark the  $\text{R}^{2+} + 2\text{R}^{5+} \rightleftharpoons 3\text{R}^{4+}$  substitution trend in columbite-type phases.

remaining vacancies were assumed to be located at the C-site. Following the above procedure, the formulae of the analyzed wodginites can be written



Changes in chromophore concentrations throughout the color gradation described above are relatively small, in-

volving a decrease in total Fe with decreasing intensity of color. Variations in Ti appear to be erratic, possibly influenced by the relatively large analytical error at the low concentration levels encountered. The Ta/(Ta + Nb) ratio seems to be rather stable, and the Sn/(Ta + Nb) ratio changes erratically (although it may be significant that it increases in the crystal terminations coexisting with discrete cassiterite grains or containing possibly exsolved cassiterite).

Unit cell dimensions of all color varieties show the  $\beta$  angle deviating appreciably from 90° (Table 3), and they change only slightly after heating at 1000°C/16 hrs. in air.

Table 2. Electron microprobe analyses of the Nb, Ta, Sn-bearing minerals from the Peerless Pegmatite

Sample number	Ta <sub>2</sub> O <sub>5</sub>	Nb <sub>2</sub> O <sub>5</sub>	TiO <sub>2</sub>	SnO <sub>2</sub>	Fe <sub>2</sub> O <sub>3</sub>	FeO	MnO	Total
A1(ct)	9.7	70.0	0.2	0.01	-	8.2	11.8	99.91
A2(ct)	9.5	70.2	0.1	0.05	-	8.02	11.9	99.77
A3(ct)	32.1	49.8	0.4	-	-	8.6	9.9	100.8
A4(ct)	11.1	69.8	0.4	-	-	8.0	12.7	102.0
A5(ct)	24.0	56.5	0.6	-	-	12.3	8.0	101.4
B1(ct)	49.6	33.3	0.3	-	-	6.0	11.2	100.4
B2(ct)	60.4	23.5	-	0.3	-	3.1	12.7	100.0
B3(ct)	61.8	22.3	0.1	0.2	-	2.8	13.0	100.2
B4(ct)	62.0	21.0	0.2	0.4	-	2.0	13.9	99.5
C1(ct)	59.4	22.7	0.6	0.9	-	6.4	9.2	99.2
C2(ct)	57.2	24.4	0.4	1.5	-	10.8	4.6	98.9
D1(ct)	72.0	11.3	0.6	0.5	-	3.2	11.9	99.5
C1(c)	1.1	0.7	0.1	97.7	-	0.3	0.03	99.93
C2(c)	2.9	0.5	0.06	94.7	-	0.4	-	98.56
C3(c)	2.5	0.7	0.1	96.7	-	0.2	-	100.2
C4(c)	4.2	0.3	-	94.9	-	0.8	-	100.2
D1(c)	11.7	0.7	0.1	85.0	-	1.4	0.3	99.2
D3(c)	0.6	-	-	99.1	-	-	-	99.7
C3(t)	75.5	8.7	0.8	2.7	-	12.8	0.3	100.8
C4(t)	71.7	11.5	0.3	1.2	-	13.8	0.9	99.4
D1(t)	80.9	4.2	0.2	2.1	-	13.3	0.6	101.3
D1(w)	62.9	5.8	0.2	18.3	0.7	1.1	9.4	98.5
D2(w) core	69.2	3.5	0.0	15.2	0.3	0.0	10.5	98.6
D2(w) margin	69.0	3.7	0.0	15.7	0.5	0.0	10.4	99.2
D3(w)	64.9	4.2	0.2	19.2	0.3	0.0	10.9	99.5
Sample number	Ta <sup>5+</sup>	Nb <sup>5+</sup>	Ti <sup>4+</sup>	Sn <sup>4+</sup>	Fe <sup>3+</sup>	Fe <sup>2+</sup>	Mn <sup>2+</sup>	Total
A1(ct)	0.615	7.383	0.035	0.001	-	1.600	2.332	11.966
A2(ct)	0.602	7.401	0.035	0.005	-	1.560	2.351	11.954
A3(ct)	2.222	5.731	0.088	-	-	1.831	2.134	11.994
A4(ct)	0.693	7.248	0.069	-	-	1.537	2.471	12.018
A5(ct)	1.596	6.247	0.110	-	-	2.515	1.657	12.126
B1(ct)	3.750	4.186	0.063	-	-	1.395	2.638	12.032
B2(ct)	4.854	3.140	-	0.035	-	0.766	3.179	11.976
B3(ct)	4.987	2.992	0.022	0.024	-	0.695	3.267	11.986
B4(ct)	5.061	2.850	0.045	0.048	-	0.502	3.534	12.040
C1(ct)	4.798	3.048	0.134	0.107	-	1.590	2.314	11.991
C2(ct)	4.598	3.261	0.089	0.177	-	2.670	1.152	11.946
D1(ct)	6.201	1.618	0.143	0.063	-	0.848	3.192	12.065
C1(c)	0.015	0.016	0.004	1.951	-	0.013	0.001	1.999
C2(c)	0.040	0.012	0.002	1.925	-	0.017	-	1.996
C3(c)	0.034	0.016	0.004	1.930	-	0.008	-	1.992
C4(c)	0.057	0.007	-	1.903	-	0.034	-	2.001
D1(c)	0.163	0.016	0.004	1.736	-	0.060	0.013	1.992
D3(c)	0.008	-	-	1.990	-	-	-	1.998
C3(t)	3.264	0.625	0.096	0.171	-	1.702	0.040	5.899
C4(t)	3.101	0.827	0.036	0.076	-	1.835	0.121	5.996
D1(t)	3.599	0.311	0.025	0.137	-	1.820	0.083	5.974
D1(w)	7.408	1.136	0.065	3.160	0.228	0.398	3.448	15.844
D2(w) core	8.323	0.700	0.000	2.680	0.100	0.000	3.933	15.736
D2(w) margin	8.227	0.733	0.000	2.745	0.165	0.000	3.862	15.732
D3(w)	7.627	0.821	0.065	3.308	0.098	0.000	3.990	15.907

Atomic contents are based on 24, 4, 12 and 32 oxygens for columbite-tantalite (ct), cassiterite (c), tapiolite (t) and wodginite (w), respectively.

This behavior suggests that the natural material is well ordered, with cation distributions close to the fully ordered formulae presented above.

### Columbite-tantalite

Columbite-tantalite crystals appear in two main forms: thin but sizeable plates within the albitic unit, and thick tabular to stumpy crystals closer to the outer margin of this unit (associations A and B, Table 1). In both types of crystals, the mineral appears homogeneous, having no significant chemical zoning, nor containing any inclusions or exsolution lamellae of other oxide minerals. Samples A have the composition of ferrocolumbite to manganocolumbite, samples B straddle the manganocolumbite-manganotantalite boundary (Figs. 1 and 2, Table 2).

The unit cell dimensions of both A and B types indicate considerable degrees of (Fe, Mn)-(Nb, Ta) disorder. Heating at 1000°C in air for 16 hrs. leads to near complete ordering of the structure, in accord with the almost ideal stoichiometry and low content of quadrivalent cations (Fig. 3, Table 3).

The only other types of columbite-tantalite found in the course of the present study are associated with cassiterite.

### Cassiterite

Cassiterite is the main oxide mineral in the cleavelandite + muscovite fringe of the albitic unit (association C, Table 1). Its composition is highly variable, containing a total of 1.71 to 14.17 wt.% of Nb, Ta, Fe and Mn oxides (Table 2). Within the limits of experimental error, all compositions appear to fall on the  $(\text{Fe, Mn})^{2+} + 2(\text{Nb, Ta})^{5+} \rightleftharpoons 3(\text{Sn, Ti})^{4+}$  trend (Fig. 2).

Microscopic grains of ferrotantalite and manganotantalite are observed dispersed along fractures in cassiterite or within the cassiterite crystals, texturally resembling exsolution bodies (Table 2, Fig. 1). Tapiolite is also found as an

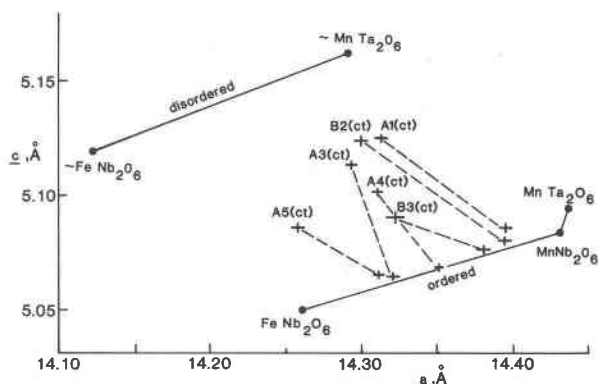


Fig. 3. Unit cell dimensions of columbite-tantalite in the  $a - c$  plot modified from Černý and Turnock (1971). All data based on the ordered supercell. Unit cell dimensions of the structural end members after Černý and Ercit (1985). Data for natural samples (with sample numbers) linked with values after heating at 1000°C/16 hrs. in air (unmarked).

Table 3. Unit cell dimensions of columbite-tantalites and wodginites from the Peerless Pegmatite

Sample number	a, Å	b, Å	c, Å	$\beta$	$V, \text{Å}^3$
Natural					
A3(ct)	14.295(2)	5.729(1)	5.113(2)	-	418.72(12)
A4(ct)	14.311(2)	5.742(1)	5.101(1)	-	419.16(8)
A5(ct)	14.258(2)	5.731(1)	5.086(1)	-	415.59(11)
B2(ct)	14.300(3)	5.741(1)	5.124(1)	-	420.61(12)
B3(ct)	14.323(4)	5.745(2)	5.090(3)	-	418.83(21)
B4(ct)	14.322(3)	5.743(2)	5.125(1)	-	420.39(12)
D1(w)*	9.552(12)	11.476(6)	5.123(3)	90°50'(5)	561.5(7)
D2(w)	9.533(1)	11.471(1)	5.117(1)	91°10'(0.6)	559.5(11)
D3(w)	9.533(2)	11.471(2)	5.116(1)	91°12'(0.9)	559.4(1)
Heated					
A3(ct)	14.320(4)	5.741(2)	5.065(1)	-	416.37(14)
A4(ct)	14.352(2)	5.745(1)	5.068(1)	-	417.89(7)
A5(ct)	14.311(3)	5.738(1)	5.065(1)	-	415.95(11)
B2(ct)	14.395(4)	5.754(1)	5.081(2)	-	420.84(16)
B3(ct)	14.381(4)	5.750(2)	5.076(1)	-	419.71(15)
B4(ct)	14.396(4)	5.757(1)	5.085(2)	-	421.48(15)
D1(w)	-	-	-	-	-
D2(w)	9.526(2)	11.474(2)	5.116(1)	91°12'(1.2)	559.1(1)
D3(w)	9.531(3)	11.465(2)	5.118(1)	91°13'(1.2)	559.2(2)

\* Gandolfi camera

apparent exsolution product, but only in cassiterite which does not carry any columbite-tantalite phase.

### Tapiolite

Microscopic crystals of tapiolite occur along the cassiterite-wodginite contacts and on the surfaces of wodginite crystals in association D, and as rounded blebs in cassiterite C. Tapiolite C is probably formed by exsolution and recrystallization, whereas primary crystallization following the precipitation of wodginite is evidently the origin of association D. Tapiolite was recognized by its optical properties and faint diffraction lines in some cassiterite X-ray patterns, and confirmed by electron microprobe analysis (Table 2). All three analyzed grains contain little Mn and are relatively enriched in Nb (Fig. 1).

### Microlite

Tiny octahedra of pale-grey microlite are rarely found on the surface of wodginite D3w. Microlite was identified by X-ray diffraction but was not found in polished sections, thus its chemical composition could not be established. However, it is suggested that the Ta/(Ta + Nb) ratio of this microlite is the same or higher than that of the associated wodginite, as is commonly found in microlites at other localities (e.g., Vormá and Siivola, 1967 and Grice et al. 1972).

### Paragenetic and geochemical considerations

As is evident from Table 1 and Figure 1, a distinct mineral succession and geochemical trend can be recognized from the inner parts of the albitic unit toward its margin along the massive quartz. A ferrocolumbite  $\rightarrow$  manganocolumbite  $\rightarrow$  manganotantalite sequence is followed by cas-

siterite and (probably minor) wodginite + microlite. This mineral succession is marked by an extensive Nb-Ta fractionation covering 85% of the total Ta/(Ta + Nb) range, and a less spectacular but distinct Fe-Mn fractionation in the Nb, Ta-rich minerals. The extent of Ta-Nb fractionation displayed here in a single unit (of a pegmatite consisting of 11 units) is rarely documented from complete border → core → replacement sequences of other pegmatites, or from entire pegmatite groups (e.g., Černý et al., 1981b; Anderson, 1983; Černý and Ercit, 1985).

With regard to the exsolution phenomena, cassiterite + tapiolite pairs show erratic and generally restricted partitioning of Fe, Mn, Nb and Ta. In contrast, columbite exsolved from cassiterite is considerably enriched in Mn, and in most cases also in Nb (samples D1, C2). The Ta-enrichment shown by tantalite C1(ct) relative to its cassiterite host is surprising, in view of the general preference of Nb for the columbite structure (e.g., Weitzel, 1976; Černý et al., 1981a). From the distribution of compositions in Figure 1 it appears that the assemblage D could have approached equilibrium much closer than any of the mineral pairs of assemblage C.

Another point of interest is the precipitation of wodginite in the cassiterite-rich margins of the albitic unit. This is undoubtedly the consequence of oversaturation of the parent environment with tin, but the reasons for crystallization of wodginite rather than ixiolite, staurigite, thoreaulite + manganotantalite or cassiterite + manganotantalite are not known. Detailed analysis of natural assemblages bearing these species, and extensive experimental studies are required to clarify this question.

### Acknowledgments

This study was supported by the NSERC of Canada Operating Grant A-7948, and by the DEMR of Canada Research Agreement 294-1983, granted to P. Černý. We are indebted to Dr. F. C. Hawthorne and Ms. K. J. Olson for helpful discussions, help in experimental work and critical reading of the manuscript. Thorough reviews by Drs. M. Ross, D. E. Voigt and E. E. Foord considerably improved the presentation.

### Note added in press

Mr. Richard Schooner of Woodstock, CT found wodginite in 1981 or 1982 in the Strickland Quarry, Connecticut pegmatite. He provided us with several crystals, associated with manganotantalite, that proved to be Ti-enriched in central parts and Ti-poor in (the margins): MnO 11.0 (10.6), Fe<sub>2</sub>O<sub>3</sub> 0.8(1.0), TiO<sub>2</sub> 0.9(0.5), SnO<sub>2</sub> 15.3(16.4), Nb<sub>2</sub>O<sub>5</sub> 4.4(3.8), Ta<sub>2</sub>O<sub>5</sub> 66.1(66.0), total 98.6(98.2) wt.%. Core Mn<sub>4.05</sub>(Sn<sub>2.64</sub>Ta<sub>0.67</sub>Ti<sub>0.30</sub>Fe<sub>0.28</sub><sup>3+</sup>)<sub>Σ3.89</sub>(Ta<sub>7.14</sub>Nb<sub>0.86</sub>)<sub>Σ8.00</sub>O<sub>32</sub>, margins Mn<sub>3.93</sub>(Sn<sub>2.86</sub>Ta<sub>0.62</sub>Fe<sub>0.33</sub><sup>3+</sup>Ti<sub>0.16</sub>)<sub>Σ3.97</sub>(Ta<sub>7.26</sub>Nb<sub>0.74</sub>)<sub>Σ8.00</sub>O<sub>32</sub>. Unit cell dimensions (single-crystal diffractometer) are *a* 9.522(1), *b* 11.467(2), *c* 5.115(1)Å, β 91.118(2)°. Data on "Monoclinic ixiolite", recently recognized to be disordered wodginite, from Alabama were presented by Foord et al. (Foord, E.E., Allen, M.S., and Heyl, A.V.: Internat. Symposium "Mineralogy in the Earth Sciences and in Industry", Toulouse 1984, Abstr.

p. 19). The mineral is under further study by T.S.E. and E.E.F.

### References

- Anderson, A. J. (1983) The geochemistry, mineralogy and petrology of the Cross Lake pegmatite field, central Manitoba. M.Sc. thesis, University of Manitoba, Winnipeg.
- Appleman, D. E. and Evans, H. T., Jr. (1973) Job 9214: indexing and least-squares refinement of powder diffraction data. U.S. Geological Survey, Computer Contributions, 20; NTIS Document PB2-16188.
- Burt, D. M. and London, D. (1982) Subsolidus equilibria. Mineralogical Association of Canada Short Course Handbook, 8, 329-346.
- Černý, P. and Ercit, T. S. (1985) Some recent advances in the mineralogy and geochemistry of Nb and Ta in rare-element granitic pegmatites. Bulletin de Minéralogie, 109, in press.
- Černý, P., Paul, B. J., Hawthorne, F. C. and Chapman, R. (1981a) A niobian rutile-disordered columbite intergrowth from the Huron Claim pegmatite, southeastern Manitoba. Canadian Mineralogist, 19, 541-548.
- Černý, P., Trueman, D. L., Ziehlke, D. V., Goad, B. E. and Paul, B. J. (1981b) The Cat Lake-Winnipeg River and the Wekusko Lake pegmatite fields, Manitoba. Manitoba Mineral Resources Division, Economic Geology Rept., ER80-1.
- Černý, P. and Turnock, A. C. (1971) Niobium-tantalum minerals from granitic pegmatites at Greer Lake, southeastern Manitoba. Canadian Mineralogist, 10, 755-772.
- Colby, J. W. (1980) MAGIC V—a computer program for quantitative electron-excited energy dispersive analysis. In: QUANTEX—Ray Instruction Manual, KEVEX corporation, Foster City.
- Ferguson, R. B., Hawthorne, F. C. and Grice, J. D. (1976) The crystal structures of tantalite, ixiolite and wodginite from Bernic Lake, Manitoba. II. Wodginite. Canadian Mineralogist, 14, 550-560.
- Grice, J. D., Černý, P. and Ferguson, R. B. (1972) The Tanco-pegmatite at Bernic Lake, Manitoba. II. Wodginite, tantalite, pseudo-ixiolite and related minerals. Canadian Mineralogist, 11, 609-642.
- v. Knorring, O., Sahama, Th. G. and Lehtinen, M. (1969) Ferroan wodginite from Ankole, southwest Uganda. Bulletin of the Geological Society of Finland, 41, 65-69.
- Rucklidge, J. and Gasparrini, E. (1969) Electron microprobe analytical data reduction (EMPADR VII). Dept. Geology, University of Toronto.
- Sheridan, D. M., Stephens, H. G., Staatz, M. H. and Norton, J. J. (1957) Geology and beryl deposits of the Peerless pegmatite, Pennington County, South Dakota. U.S. Geological Survey Professional Paper, 297-A.
- Turnock, A. C. (1966) Synthetic wodginite, tapiolite and tantalite. Canadian Mineralogist, 8, 461-470.
- Vorma, A. and Siivola, J. (1967) Sukulaite-Ta<sub>2</sub>Sn<sub>2</sub>O<sub>7</sub>-and wodginite as inclusions in cassiterite in the granite pegmatite in Sukula, Tammela, in S.W. Finland. Bulletin de la Commission Géologique de Finlande, 229, 173-187.
- Weitzel, H. (1976) Kristallstrukturverfeinerung von Wolframiten und Columbiten. Zeitschrift für Kristallographie, 144, 238-258.
- Wise, M. A. and Černý, P. (1984) First U.S. occurrence of wodginite from Powhatan County, Virginia. American Mineralogist, 69, 807-809.

Manuscript received, December 27, 1983;  
accepted for publication, February 19, 1985.